applied sciences

MDPI

Article

The Enhancement Discharge Performance by Zinc-Coated Aluminum Anode for Aluminum–Air Battery in Sodium Chloride Solution

Ruly Bayu Sitanggang [1,*], Syarifa Nur'aini [2], Susanto Susanto [2], Widiyastuti Widiyastuti [2] and Heru Setyawan [2]

[1] PT. PLN (Persero) Center for Electricity Research and Development, Jl. Duren Tiga No. 102, Pancoran, Jakarta Selatan 12760, Indonesia
[2] Department of Chemical Engineering, Faculty of Industrial Technology and System Engineering, Institut Teknologi Sepuluh Nopember, Kampus ITS Sukolilo, Surabaya 60111, Indonesia
* Correspondence: rully.bs@pln.co.id

Abstract: The main drawback of seawater batteries that use the aluminum (Al)–air system is their susceptibility to anode self-corrosion during the oxygen evolution reaction, which, in turn, affects their discharge performance. This study consist of an electrochemical investigation of pure Al, 6061 Al alloy, and both types coated with zinc as an anode in a 3.5% sodium chloride (NaCl) electrolyte. The electrolyte solution used for the deposition of zinc metal contained citrate, with and without EDTA as a complexing agent. Subsequently, the performance of the anode was tested in a seawater battery, using a carbon@MnO_2 cathode and a 3.5% NaCl electrolyte. The performance of Al–air batteries has been significantly enhanced by applying a process of electrodepositing zinc (Zn) with a citrate deposition electrolyte solution in both pure aluminum and alloy 6061. The performance of the battery was further enhanced by adding EDTA as a chelating agent to the citrate-based electrolyte solution. The Al–air battery with aluminum alloy 6061 with Zn electrodeposition with an additional EDTA as the anode, carbon@MnO_2 as the cathode, and NaCl 3.5% solution as the electrolyte has the highest battery performance, with a specific discharge capacity reaching 414.561 mAh.g^{-1} and a specific energy density reaching 0.255 mWh.g^{-1}, with stable voltage at 0.55 V for 207 h.

Keywords: aluminum; coating; electrodeposition; seawater battery

check for updates

Citation: Sitanggang, R.B.; Nur'aini, S.; Susanto, S.; Widiyastuti, W.; Setyawan, H. The Enhancement Discharge Performance by Zinc-Coated Aluminum Anode for Aluminum–Air Battery in Sodium Chloride Solution. *Appl. Sci.* **2024**, *14*, 6263. https://doi.org/10.3390/app14146263

Received: 17 April 2024
Revised: 21 June 2024
Accepted: 21 June 2024
Published: 18 July 2024

Copyright: © 2024 by the authors. Licensee MDPI, Basel, Switzerland. This article is an open access article distributed under the terms and conditions of the Creative Commons Attribution (CC BY) license (https://creativecommons.org/licenses/by/4.0/).

1. Introduction

The increasing focus on sustainable and eco-friendly energy sources has increased the investigation of energy storage technologies. Among these, aluminum (Al) air batteries have emerged as significant candidates [1], mainly due to their high energy density and the use of aluminum metal as an anode. Aluminum's abundance, affordability, safety, and sustainability make it an attractive choice [2]. However, despite these benefits, Al–air batteries face challenges associated with the generation of byproducts at the interface between the anode and the electrolyte. Furthermore, the inherent protective oxide film of aluminum impedes electron conduction in many aqueous environments, thus increasing the overvoltage of anodic dissolution [3] and causing delays in anode activation [4]. These challenges compromise the performance and efficiency of Al–air batteries.

Aluminum batteries have been extensively investigated, particularly with a focus on their application in alkaline solutions. Studies have compared the performance of aluminum batteries using different grades of aluminum, such as commercial and pure grades, within 4M NaOH electrolytes in Al–air battery systems [5]. The choice of electrolyte is crucial in aluminum–air batteries, and most studies use aqueous alkaline solutions, which can cause leakage or short circuits under bending or stretching conditions [6]. Despite the advantages of Al–air batteries, such as a high theoretical energy density and low cost,

self-discharge of the aluminum anode in alkaline solutions remains a challenge, affecting the utilization rate [7]. The use of seawater or neutral salts as electrolytes in metal–air batteries is considered a viable and sustainable option, increasing its appeal and potential for future development [8–10]. Researchers have explored various strategies to address the corrosion of aluminum anodes in alkaline solutions, including inhibiting self-corrosion through different methods [11]. Furthermore, the use of additives such as L-cysteine/zinc oxide has been determined to influence the electrochemical behavior of pure aluminum in alkaline solutions [7]. Furthermore, the formation of protective layers on the surface of the aluminum anode has been proposed as a means of effectively inhibiting corrosion [12]. In pursuit of more efficient and safer battery systems, the development of alternative battery technologies with improved safety and cost effectiveness is a significant area of focus [13]. Studies have also examined the impact of electrolyte additives, such as agar, on the performance of aluminum–air batteries [14]. Furthermore, the synergistic effect of different compounds, such as potassium sodium tartrate tetrahydrate and sodium stannate trihydrate, has been explored to inhibit aluminum self-corrosion in alkaline aluminum–air batteries [15].

The use of commercial-grade aluminum as an anode material in high-power discharge conditions in Al–air batteries has been supported by various studies. Commercial grade aluminum has been found to exhibit higher open-circuit potential and corrosion rates compared to pure-grade aluminum, making it a viable and cost-effective option for such applications [16]. Efforts to suppress parasitic corrosion in aluminum–air batteries include doping high-purity-grade aluminum with specific alloying elements and introducing corrosion inhibitors into the electrolyte [17]. Studies have shown that aluminum corrosion behavior can be influenced by various factors, such as the presence of alloying elements such as magnesium (Mg) and silicon (Si), which can affect corrosion rates in different environments [18]. Furthermore, atmospheric conditions, including the presence of chloride and sulfate ions, can significantly affect the corrosion rate of aluminum [17,19]. The addition of certain additives, such as L-Cysteine/zinc oxide, has been found to influence the electrochemical behavior of aluminum in alkaline solutions, potentially affecting its corrosion properties [7]. Furthermore, the use of inhibitors such as sulfathiazole has been investigated for their effectiveness in inhibiting aluminum corrosion in specific environments, highlighting the importance of corrosion inhibition strategies in maintaining the integrity of aluminum materials [20]. Furthermore, the presence of ceramic particles as additives has been shown to impact the electrochemical behavior of aluminum, potentially affecting its corrosion resistance as a galvanic anode in Al–air batteries [21].

Incorporating an aluminum alloy significantly lowers the corrosion rate, thereby prolonging the operational life of aluminum–air batteries. In addition, the introduction of small amounts of certain metals into an alkaline medium has been explored and found to harness synergistic effects that improve the performance of aluminum alloys [16,22–25]. However, aluminum reacts rapidly and irreversibly with oxygen, forming a stable oxide layer that critically affects its electrochemical behavior in aqueous electrolytes. Introducing specific metals into aluminum alloys and using a 2M NaCl electrolyte can improve voltage performance [26]. The corrosion resistance of these aluminum alloys has been evaluated in different electrolytic media to determine their inhibitory effects [27–29]. The integration of small metal concentrations into aluminum alloys has been shown to enhance current capacity and corrosion inhibition [8]. However, investigations on the corrosion behavior of metal-coated aluminum plates in the NaCl electrolyte of 3.5%, a surrogate for seawater, have been limited and have not been applied as anode material in aluminum–air batteries [30,31]. In addition to utilizing aluminum metal alloys to enhance anode characteristics, the deposition of metals onto pure aluminum or its alloys has also been explored. Specifically, the deposition of copper on the anode has been shown to improve the efficiency of the anode. Furthermore, copper deposited in the 7075 aluminum alloy through electrochemical and chemical deposition processes exhibits greater stability than copper deposited on pure aluminum. In particular, the electrochemical deposition process has been found to be more

efficient, economical, and practical compared to the chemical deposition method, and in some cases, chemical deposition may not even be feasible [32–34].

Other metals, such as zinc, have been identified as potential corrosion inhibitors by forming a protective coating on the substrate surface, thus improving the performance of aluminum as an anode in metal–air batteries [35]. Therefore, this research intends to study and contrast the electrochemical behavior of two varieties of aluminum—the unalloyed alloy and the 6061 alloy—in Al–air batteries, deposited with zinc and employing a 3.5% sodium chloride solution as an alternative to seawater. Furthermore, the procedure of depositioning zinc on the aluminum surface was investigated with and without the incorporation of the EDTA complexing agent during electrodeposition to assess its influence on the performance of the anode.

2. Materials and Methods

2.1. Materials

This study obtained two types of aluminum under investigation, which were high-purity aluminum from Merck (98% purity) and the commercial aluminum alloy 6061. For the deposition materials, they consisted of zinc sulfate pentahydrate ($ZnSO_4.7\,H_2O$, reagent grade), trisodium citrate dihydrate ($C_6H_5Na_5O_7.2\,H_2O$, reagent grade), and ethylenediaminetetraacetic acid, known as EDTA ($C_{10}H_{16}N_2O_8$, reagent grade). All electrolyte bath materials for deposition were purchased from Merck, Singapore. The cathode materials were applied in commercial nickel foam, coated with carbon black acetylene from MTI Corporation and MnO_2 from Inoxia, United Kingdom. Commercial MnO_2, as an electrocatalyst, is α-MnO_2 type, 45 µm in size, with $\geq$80% purity. For the electrochemical performance test, sodium chloride (NaCl, reagent grade) was used from Merck, Singapore, as the electrolyte material.

2.2. Anode Sysnthesis

The electrodeposition process for the zinc (Zn) material aimed to coat a 1×1 cm^2 area on each aluminum-type surface using two different methods. The specific compositions of the aluminum used as the anode are detailed in Table 1. The initial step involved the preparation of the bath by heating deionized water to 80 °C, followed by the sequential addition of all bath materials, as outlined in Table 2. The solution was continuously stirred until a homogeneous and transparent electrolyte solution was achieved. The entire electrodeposition process was carried out for a duration of 15 min, using a platinum (Pt) wire as the counter cathode, with a maintained electrode distance of 10 mm.

As a result of the slower deposition rate observed in the second method, the current density is adjusted to higher levels than in the first method. Consequently, the current density was maintained at 11 mA cm^{-2} for the first method and increased to 300 mA cm^{-2} for the second to compensate for the reduced deposition rate and ensure efficient coating.

Table 1. Elemental composition of aluminum selected for the anode.

Element	Pure Al % wt.	Al Alloy AA6061 % wt.
Al (Aluminum)	~100	97
Si (Silicon)	≤0.5	0.73
Mn (Manganese)	≤0.01	0.08
Zn (Zinc)	≤0.05	0.01
Ni (Nickel)	-	0.015
Ti (Titania)	-	0.03
Cu (Copper)	≤0.005	0.31
Mg (Magnesium)	-	1.51
Fe (Iron)	≤1.0	0.18
Cr (Chrome)	-	0.08
N (Nitrogen total)	≤0.005	-
As (Arsenic)	≤0.0002	-

Before the electrodeposition process, the aluminum substrates must undergo pretreatment to eliminate the naturally formed oxide layer on their surface. This involves abrading the aluminum substrate with commercial emery paper (grit 2000), sonicating it in 96% ethanol for 15 min, and etching it in a solution of 0.1% sulfuric acid (H_2SO_4).

Table 2. Electrolyte bath composition for electrodeposition.

Bath Composition	$ZnSO_4$ mol L^{-1}	$C_6H_5Na_5O_7$ mol L^{-1}	$C_{10}H_{16}N_2O_8$ mol L^{-1}
First route	0.2	0.2	-
Second route	0.2	0.2	0.6

2.3. Cathode Synthesis

The nickel foam was prepared by cutting it into 1×1 cm^2 pieces, corresponding to the size of the active surface area. The cathode materials, consisting of a mixture of commercial MnO_2 from Inoxia and carbon black sourced from the MTI Corporation in a 4:1 ratio, were first combined with 10% polyvinylidene fluoride (PVDF) from Sigma-Aldrich based on their total mass. The powder mixture was then uniformly blended using ball milling. Subsequently, N-methyl-2-pyrrolidone (NMP) solvent from Sigma-Aldrich was added to the mixture and stirred until a homogeneous suspension was achieved. This slurry was applied manually to the nickel foam, ensuring even coverage. Finally, the coated nickel foam was dried in a furnace at 200 ^{o}C for 30 min to ensure proper adhesion and to remove any residual solvent.

2.4. Characterization

Scanning electron microscopy (SEM), using an FEI Inspect S50 instrument, was performed to examine the morphology and thickness of the applied coatings. Additionally, energy-dispersive X-ray spectroscopy (EDX) analyses were performed to determine the elemental composition and percentages resulting from various coating processes and on different substrate types. These techniques allowed for a detailed assessment of the surface structures and elemental makeup of the coatings, providing insights into their physical characteristics and potential performance in their respective applications.

2.5. Electrochemical Performance

Electrochemical analyses of the anodes were performed using potentiostat instrumentation (Autolab PGSTAT302N, Utrecht, The Netherlands), capable of measuring both linear polarization and cyclic voltammograms in a solution of 3.5% NaCl electrolytes at room temperature. The experimental setup included a half-cell configuration with the anode as the working electrode, Ag/AgCl as the reference electrode, and a platinum wire as the counter electrode. To ensure accurate measurements, the electrolyte solution was saturated with oxygen for 30 min prior to the tests. Polarization measurements were made at a scan rate of 10 $mV.s^{-1}$, with a potential range set to 25 mV relative to the open circuit potential (OCP), allowing for determination of the steady-state OCP value. Furthermore, the cathode materials were also subjected to cyclic voltammetry (CV) analysis using the same equipment. CV tests were carried out at a scan rate of 10 $mV.s^{-1}$, covering a potential range of -1 V to +1 V in a 3.5% NaCl electrolyte solution saturated with oxygen, and similarly under nitrogen-saturated conditions to compare the effects of different gases on electrochemical behavior. In addition to these electrochemical characterizations, a battery analyzer (BST with 8 channels, Richmond, CA, USA) was utilized to assess discharge time and quality, comprising both anode and cathode materials in a 3.5% NaCl electrolyte solution. The current density was maintained at 2 mA cm^{-2} throughout the discharge analysis, allowing for evaluation of the battery performance under controlled conditions.

3. Results and Discussion

The performance of an electrocatalyst with loading 80% MnO_2, utilized in the cathode, was evaluated to determine its electrocatalytic activity towards the oxygen reduction reaction (ORR) in a solution of 3.5% NaCl. This evaluation was conducted under room temperature conditions using CV measurements, with the solution saturated alternately with nitrogen and oxygen.

The cyclic voltammogram revealed a significant peak indicative of oxygen reduction reaction (ORR) activity in an oxygen-saturated solution, occurring at −0.427 V vs. Ag/AgCl, which is depicted as a solid line in Figure 1. In contrast, the voltammogram obtained from the nitrogen-saturated solution exhibited a flat characteristic, suggesting the absence of ORR under these conditions. Consequently, the use of an electrocatalyst containing 80% MnO_2 is validated for further investigation of battery performance, highlighting its effectiveness in facilitating ORR in environments saturated with oxygen. Pure aluminum and the aluminum alloy 6061 have been chosen as the materials for the anode. SEM images and the EDX mapping of their surfaces are presented in Figure 2. The analysis reveals that the predominant element in pure aluminum is aluminum itself, with trace elements not detected by EDX. The aluminum alloy 6061 is composed of 96% aluminum, 2% magnesium, 1% silica, and trace elements that are not identified by EDX. The elemental compositions of both pure aluminum and the aluminum alloy 6061 meet the product specifications described in Table 1.

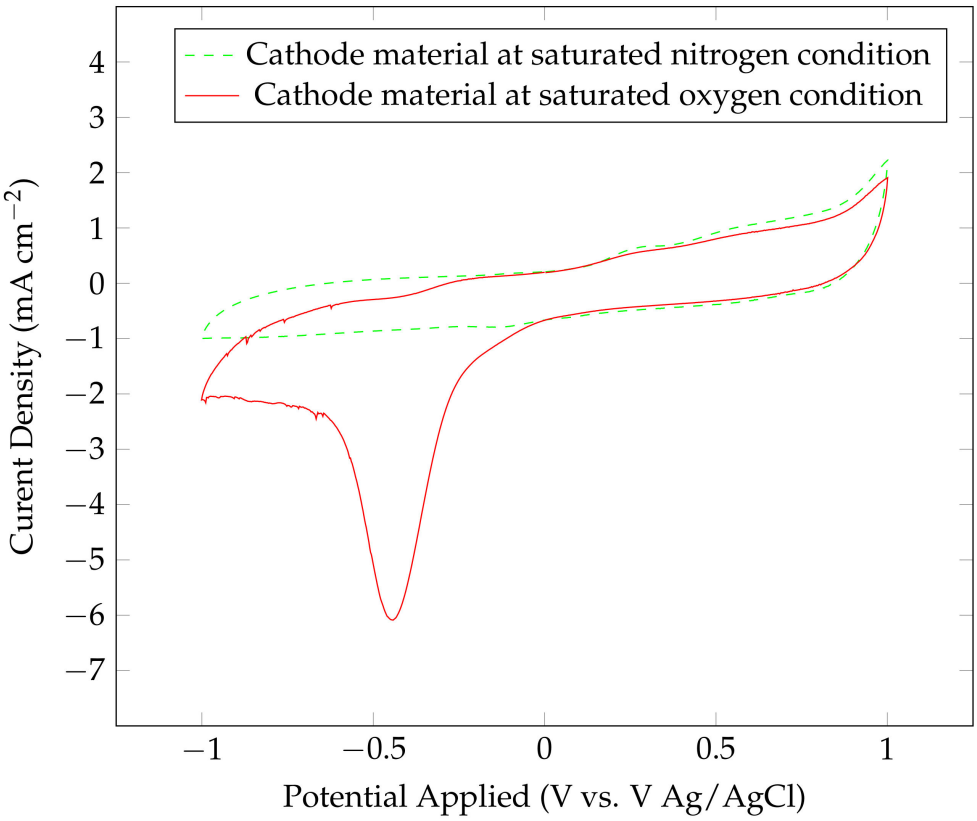
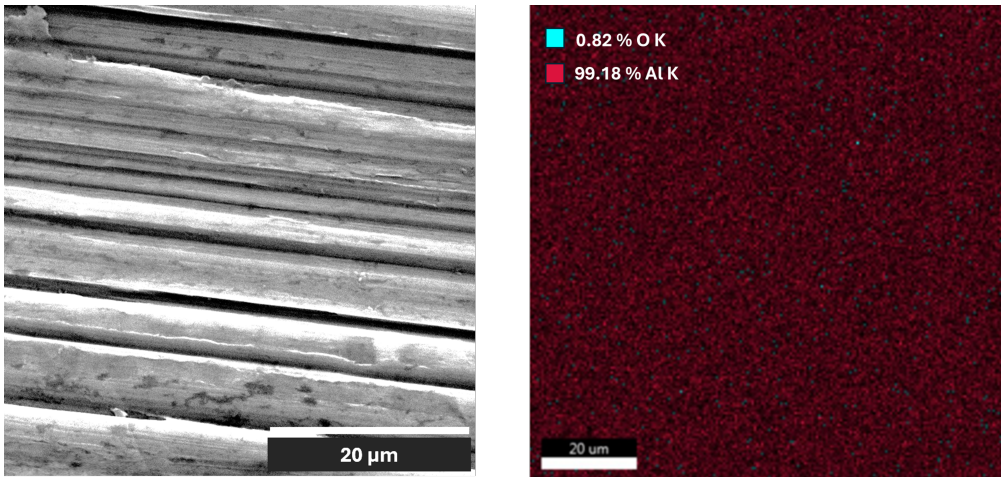
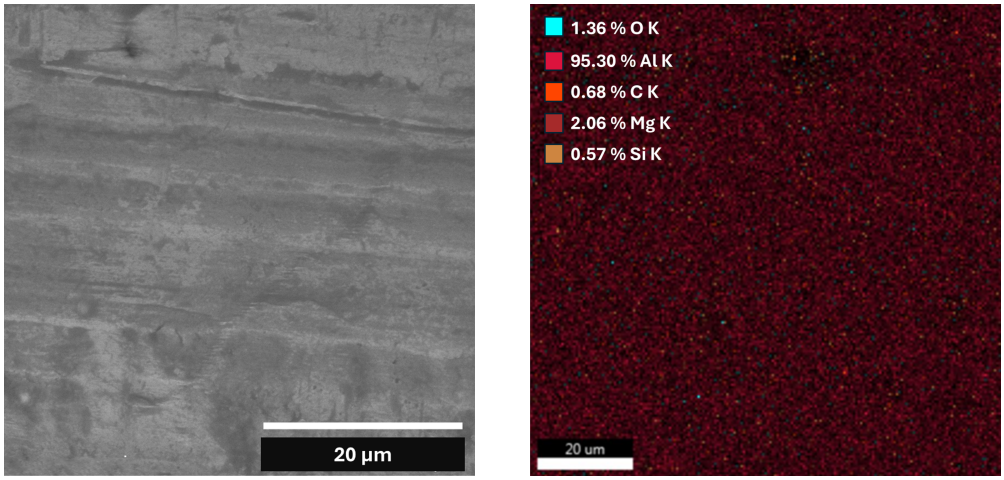


Figure 1. Voltammograms of CV for MnO_2–acetylene black = 4:1 electrocatalyst in nitrogen-saturated (dashed line) and oxygen-saturated (solid line) 3.5% NaCl solution at a scan rate of 10 mV.s^{-1}.



(**a**) Pure Al

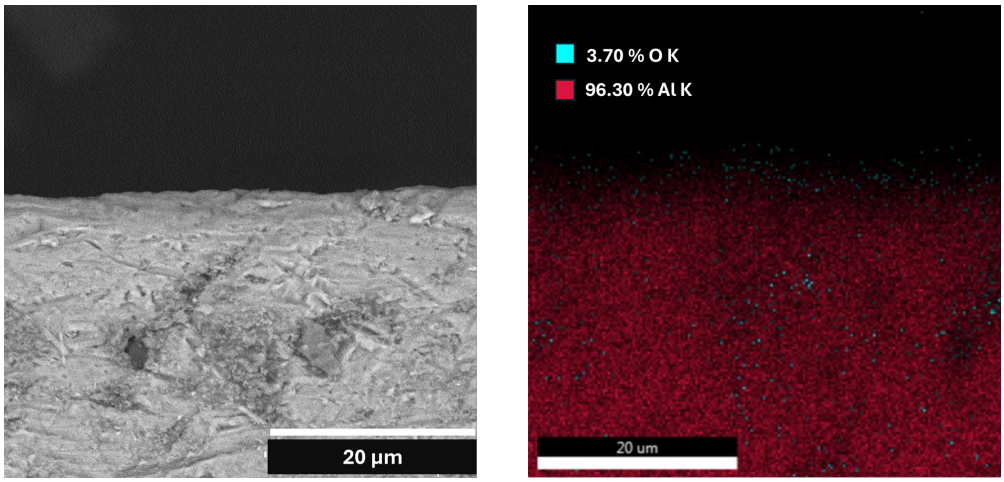


(**b**) AA 6061

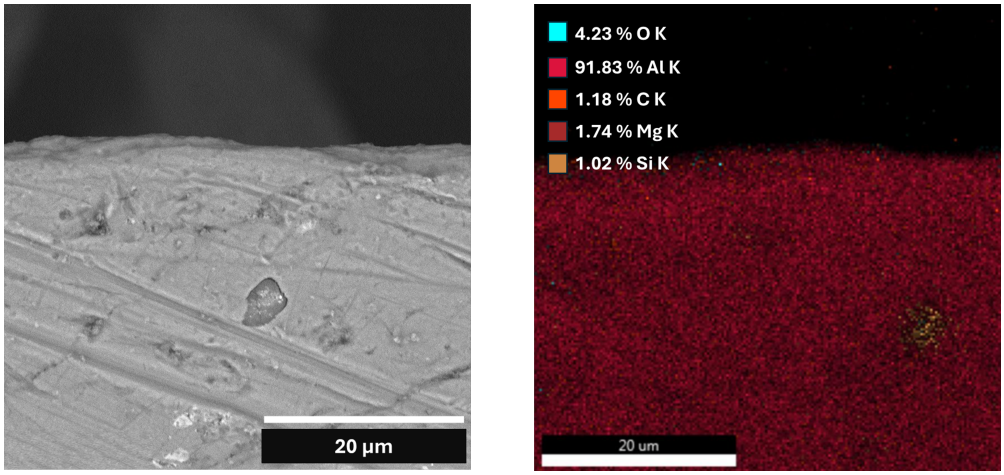
Figure 2. SEM images and EDX mapping at the surface of the anode: (**a**) pure aluminum and (**b**) aluminum alloy 6061.

The SEM images and EDX analysis of the cross-sectional areas of pure aluminum and the 6061 aluminum alloy are presented in Figure 3. The cross-sectional structure is notably consistent across both the anode surfaces of pure aluminum and the aluminum alloy 6061. Furthermore, there is no evidence of film formation or any other type of separation on the anode surfaces that could be attributed to oxide formation. The elemental composition revealed by the EDX mapping in the cross-sectional areas aligns with the product specifications, despite a minor increase in the formation of oxides.

The discharge performance of batteries using anodes made from pure aluminum and the 6061 aluminum alloy was evaluated via constant current discharge tests at 2 mA cm^{-2} in a solution of 3.5% NaCl, as illustrated in Figure 4a. The findings reveal that anodes made of pure aluminum exhibit a shorter discharge time compared to those made from the 6061 aluminum alloy. Specifically, Figure 4a shows that for pure aluminum anodes, the discharge performance is maintained. In contrast, the 6061 aluminum alloy demonstrated stable discharge performance, maintaining a relatively constant voltage of 0.55 V for 49 h, as shown in Figure 4b. The use of the 6061 aluminum alloy as an anode material resulted in an increase in discharge energy compared to pure aluminum anodes. The presence of elements such as magnesium and silica in the 6061 aluminum alloy could contribute to its improved mechanical strength and corrosion resistance. Further investigations of the passivation and corrosion resistance properties of each anode material were conducted using linear polarization techniques.

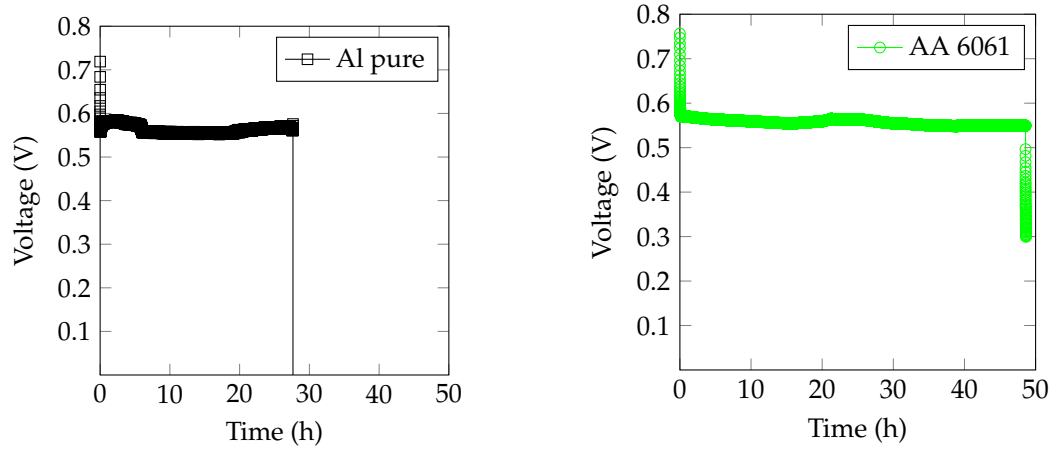


(**a**) Pure Al cross section.



(**b**) AA 6061 cross section.

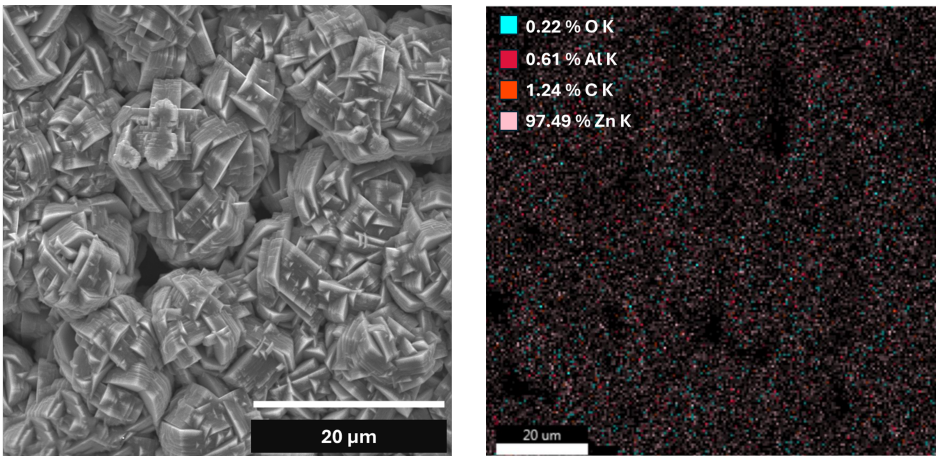
Figure 3. SEM images and EDX mapping at the cross section surface of the anode: (**a**) pure aluminum and (**b**) aluminum Alloy 6061.



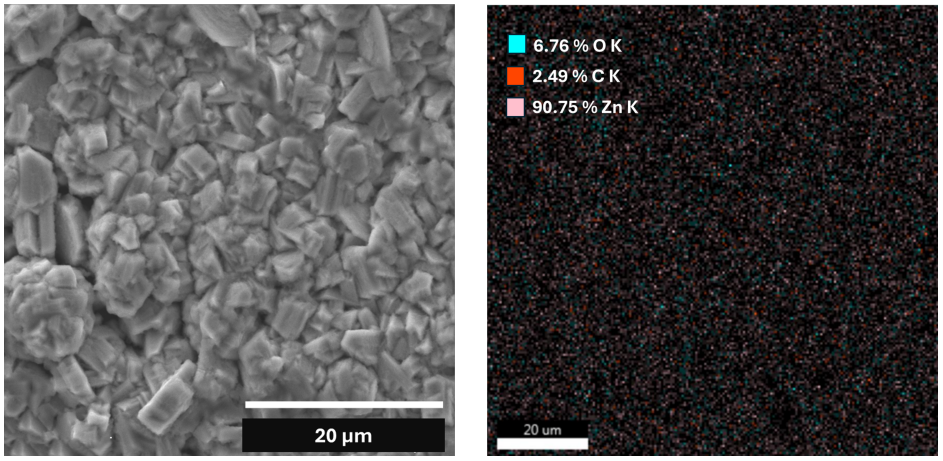
(**a**) Pure Al discharge curve. (**b**) Al 6061 discharge curve.

Figure 4. Discharge behavior of Al–air battery using (**a**) pure aluminum and (**b**) aluminum alloy 6061 at current densities of 2 mA cm^{-2}.

The impact of zinc coating on pure aluminum and the aluminum alloy 6061, applied via the electrodeposition method for use as an anode in Al–air batteries, is also investigated. Figure 5a illustrates the zinc deposition on the surfaces of pure aluminum and the 6061 aluminum alloy via electrodeposition.



(**a**) Pure Aluminum.

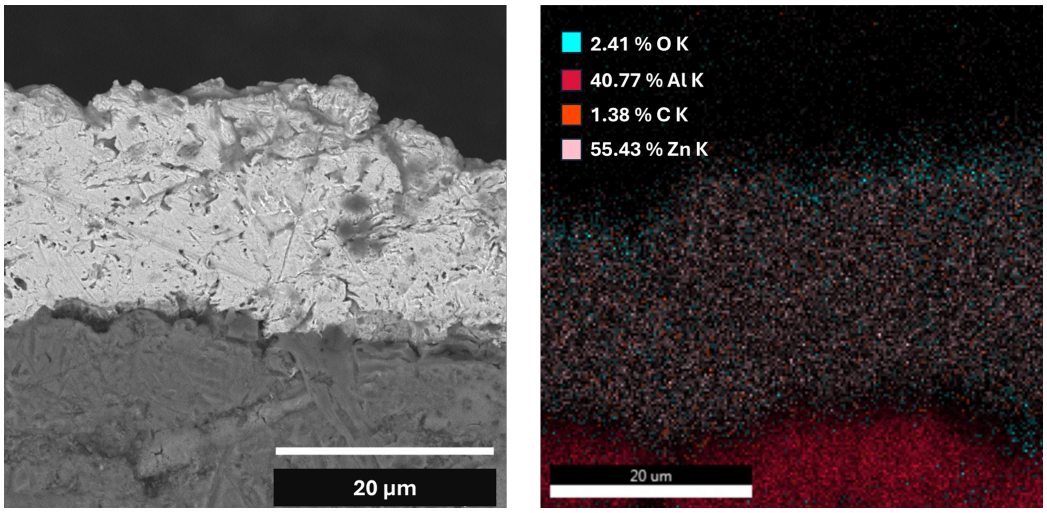


(**b**) AA 6061.

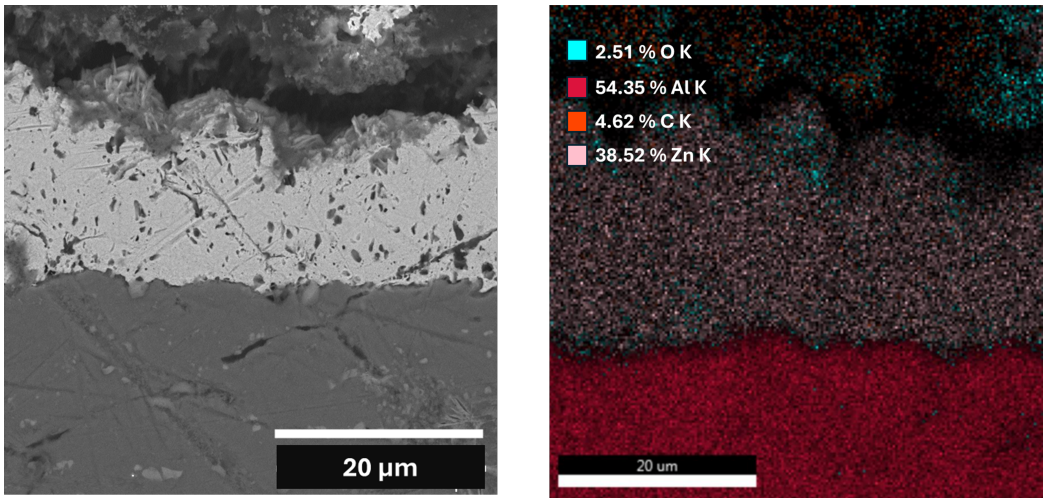
Figure 5. SEM images and EDX mapping at the surface of the zinc-coated anode—(**a**) pure aluminum and (**b**) aluminum alloy 6061—using aqueous zinc solution during electrodeposition.

It can be seen that the zinc grains on the pure aluminum (Figure 5a) are larger than those of the 6061 aluminum alloy (Figure 5b). Furthermore, there is a tendency for zinc grains in pure aluminum to undergo agglomeration. Figure 6 presents the cross-sectional views of the zinc coatings on anodes made from pure aluminum (Figure 6a) and aluminum alloy 6061 (Figure 6b), with average thicknesses measured at 20.0 µm and 17.8 µm, respectively. Zinc and its oxide, being the predominant coating materials, exhibit distinct demarcations between the zinc layer and the aluminum substrate, as evidenced by the SEM images and the EDX mapping.

The electrodeposition process, which utilizes only an aqueous zinc sulfate solution, leads to the formation of a thick layer of zinc with large grains, which can be attributable to the high rate of deposition. To moderate this deposition rate, we introduced EDTA as a chelating agent into the solution. The presence of EDTA results in the formation of Zn chelates, effectively slowing the rate of zinc deposition.



(**a**) Pure Al cross section.



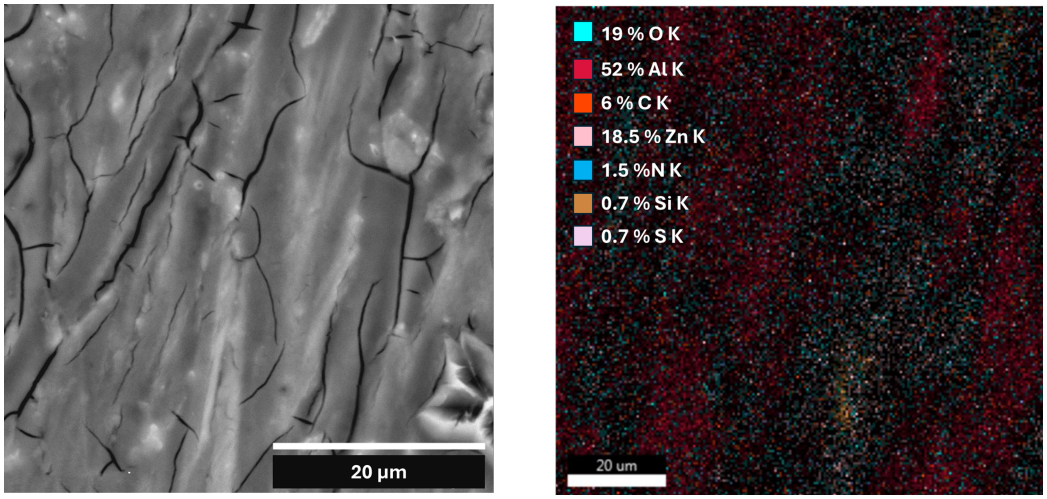
(**b**) AA 6061 cross section.

Figure 6. SEM images and EDX mapping at the cross-section of the zinc-coated anode—(**a**) pure aluminum and (**b**) aluminum alloy 6061—using aqueous zinc solution during electrodeposition.

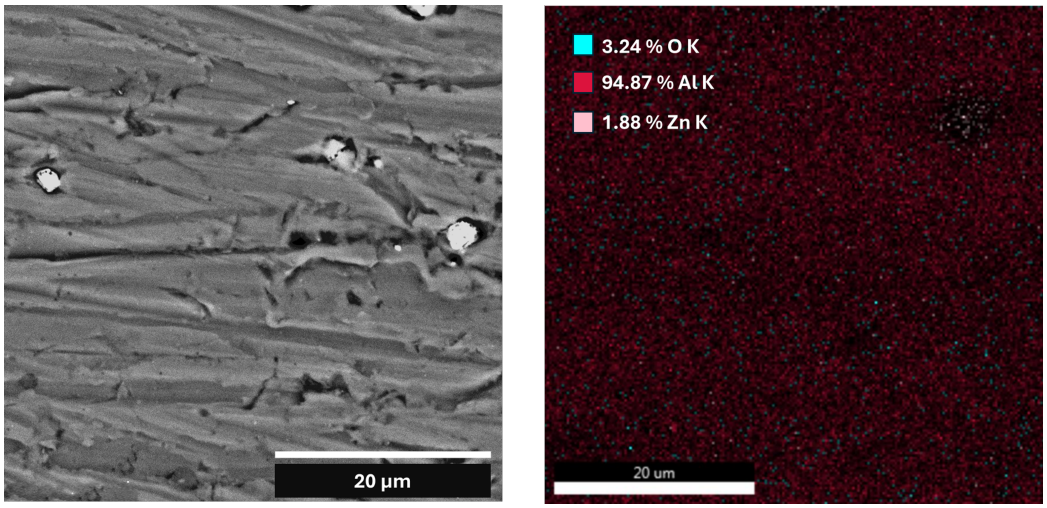
EDTA as the complexing agent will bind with the metal ion and influence its reactivity and mobility in the electrolyte. It leads to more control and uniformity of the quality of the coating, including better coating–substrate bonding, a denser layer, and improved uniformity on a complex-shaped substrate. Meanwhile, citrate based only within the electrolyte is mostly used to reduce its original compound to a metal ion [36,37].

In an aqueous electrolyte, zinc ions can form various complexes, including $Zn(H_2O)_6^{2+}$. The presence of complexing agents such as citrates or EDTA will influence the formation of these complexes and subsequently affect the deposition process. The structures of the EDTA complexes and the disodium salt of EDTA are illustrated in [38]. In the presence of complexing agents, zinc ions form stable complexes such as $Zn(EDTA)^{2-}$ or Zn(Citrate) complexes. The complexation reduces the concentration of free zinc ions, moderating the deposition rate and resulting in a finer and more uniform deposit.

Figure 7 presents the SEM images and EDX mapping of the surfaces of pure zinc-coated aluminum and the 6061 aluminum alloy, used as anodes, which were treated with EDTA in the aqueous zinc solution during the electrodeposition process. The SEM images reveal that the zinc coating appears as a thin film on the aluminum anodes. The surface structures of the zinc-coated aluminum anodes are comparable to those of the uncoated ones. In addition, the EDX mapping shows the presence of base aluminum and zinc elements.



(**a**) Pure Aluminum.



(**b**) AA 6061.

Figure 7. SEM images and EDX mapping at the surface of the zinc-coated anode—(**a**) pure aluminum and (**b**) aluminum alloy 6061—using aqueous zinc solution containing EDTA during electrodeposition.

Figure 8 illustrates the polarization curves for pure Al, Zn-pure Al, and Zn(EDTA)-pure Al anodes. In the figure, it is apparent that the pure Al anode has the most positive corrosion potential, followed by Zn-pure Al, while Zn(EDTA)-pure Al exhibits the most negative corrosion potential, as detailed in Table 3. In general, the charge transfer coefficient (α_a) indicates that a higher value leads the interfacial potential to lower the free energy that impedes electrochemical reaction. As a result, the activation overpotential is further decreased; then, current densities are improved, and the effectiveness of the electrochemical reactions is improved [39].

Furthermore, the corrosion current density (I_{corr}) increases with the application of the zinc coating. In particular, the highest I_{corr}, indicative of the best corrosion resistance, is achieved when EDTA is added during the zinc electrodeposition process. A more negative corrosion potential signifies enhanced electrochemical activity, as evidenced by the extended battery discharge time.

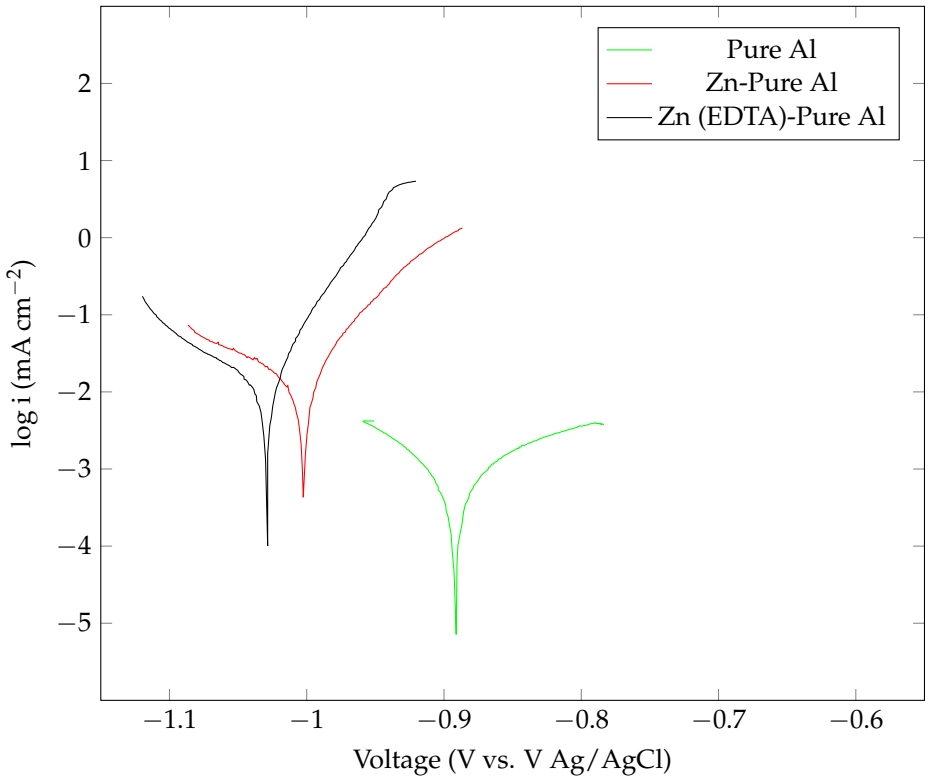


Figure 8. Polarization curves at scan rate of 10 mV.s^{-1} of pure Al, Zn-pure Al, and Zn(EDTA)-pure Al in 3.5% NaCl solution.

Table 3. Electrochemical parameters of anode samples.

Anode Sample	Icorr (μA cm^{-2})	Ecorr (V, Ag/AgCl)	α_a	Corrosion Rate (mm/year)
Pure Al	2.18	−0.912	0.323	0.025361
Zn-pure Al	16.16	−0.983	0.332	0.13666
Zn (EDTA) pure Al	18.41	−1.032	0.436	0.21395
AA 6061	29.72	−0.696	0.192	0.3454
Zn-AA 6061	72.56	−0.9466	0.252	0.84322
Zn (EDTA)-AA 6061	110.59	−0.9949	0.306	1.285

The same tendency towards polarization curves occurred with the use of the aluminum alloy 6061 anode, as shown in Figure 9. The corrosion potential shifts to a more negative value in the order of AA 6061, Zn-AA 6061, and Zn(EDTA)-AA 6061.

The higher negative corrosion potential led to better electrochemical activity. As shown in Table 3, the corrosion current density, I_{corr}, increases with the zinc coating on the surface of the aluminum alloy, then is followed by the highest value of EDTA treatment during electrodeposition of the zinc alloy. The use of the 6061 aluminum alloy gives lower corrosion resistance compared to pure aluminum.

The zinc-coated anode also decreases corrosion resistance and decreases most with EDTA treatment during the electrodeposition process, as shown in Table 3, indicated by the increase in the corrosion rate.

In addition, the deposition of zinc on the 6061 aluminum alloy results in a discharge time that exceeds that of pure aluminum, as illustrated in Figure 10b. The zinc layer, with or without EDTA addition, plays a significant role in the extended battery life for the discharging process. The deposit of a thin layer on the surface of the anode prevents the instability of the metal-based anode, including dendrite growth, metal corrosion, and interference by heteroions [40,41].

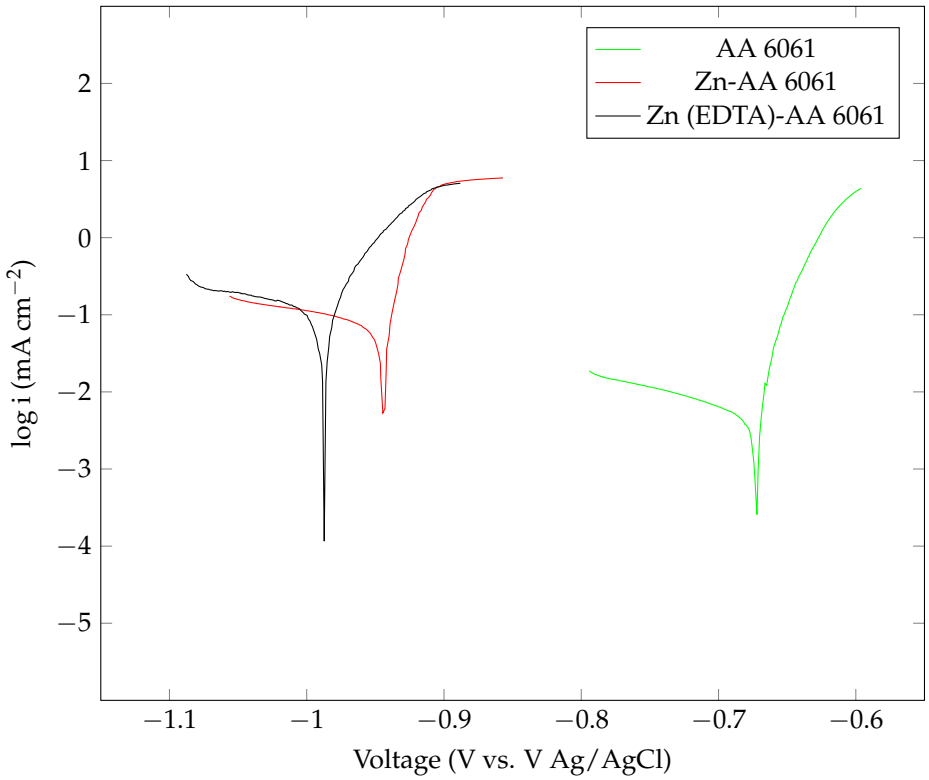


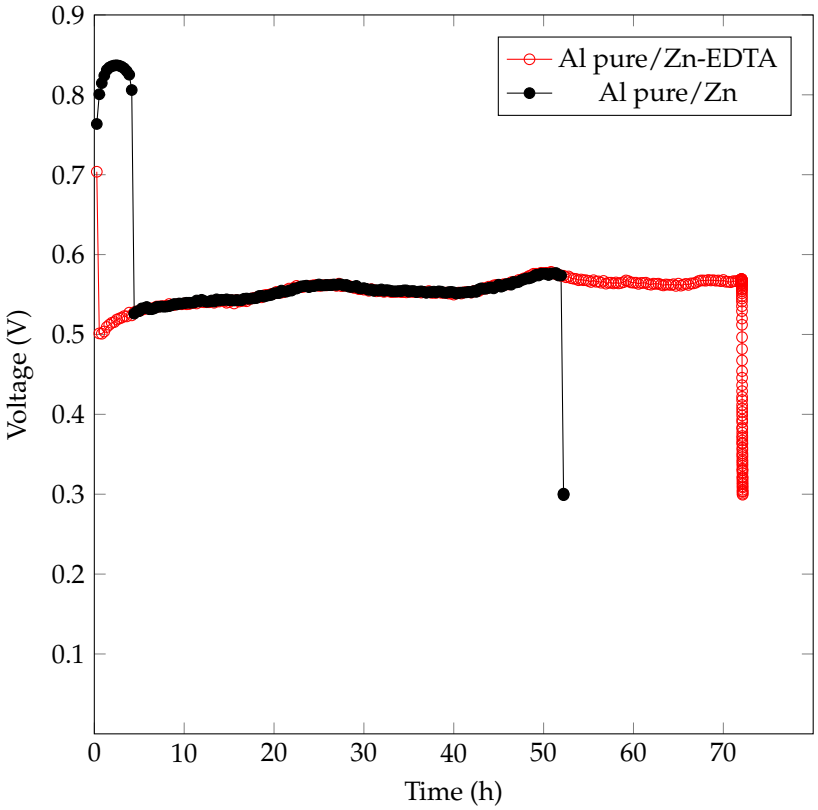
Figure 9. Polarization curves at scan rate of 10 mV.s^{-1} of AA 6061, Zn-AA 6061, and Zn(EDTA)-AA 6061 in 3.5% NaCl solution.

The discharge behavior in a 3.5% NaCl solution for pure aluminum anodes coated with zinc, with and without EDTA during electrodeposition, is shown in Figure 10a. This figure shows that the zinc coating leads to a more stable and prolonged discharge behavior compared to the scenario without the zinc coating.

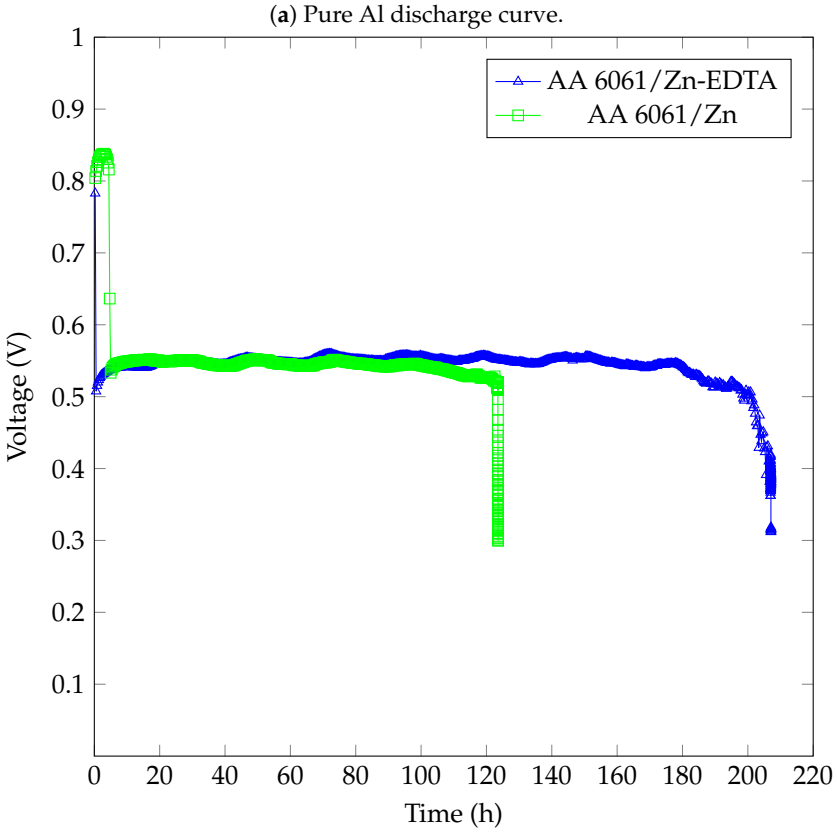
Specifically, zinc-coated pure aluminum anodes prepared with EDTA during electrodeposition exhibited a discharge duration of 72 h, exceeding the discharge time of 52 h of those prepared without EDTA, at a relatively constant voltage of 0.55 V. These findings are consistent with polarization measurements, which indicate that the incorporation of EDTA in the Zn electrodeposition process enhances electrochemical activity.

The addition of EDTA during zinc electrodeposition on the aluminum alloy anode results in the longest discharge time, extending up to 207 h, almost double the duration of the anode prepared without EDTA, which lasts up to 124 h at a relatively constant voltage of 0.55 V. The use of EDTA-assisted electrodeposition for zinc thin films yields the optimal discharge performance of the battery.

The modified anode with electrodeposition boasts a valuable improvement in comparison to the original anode. The lack of pure Al performance is caused by the oxide layer that was naturally formed. The oxide layer blocked the active surface to react with the electrolyte; therefore, the open circuit potential of the coated anode is higher than that of the initial anode. The oxide layer in coated Al is expected to be removed in a pretreatment process before electrodeposition. Then, the deposited metal is directly layered on an active Al surface. The active Al surface then reacts with the electrolyte, and the reaction that might occur between the Al and sodium chloride electrolyte is described below. For EDTA, the addition variable has more superior performance compared to the citrate-based-only example because of stronger binding and a denser coating. The larger grain of the coating in the citrate-based variable will be easier to abrade [42]. The reaction mechanism is shown in Figure 11.



(**a**) Pure Al discharge curve.



(**b**) AA 6061 discharge curve.

Figure 10. Discharge behavior of Al–air battery using zinc-coated (**a**) pure aluminum and (**b**) aluminum alloy 6061 without and with EDTA addition in the aqueous zinc solution at current densities of 2 mA cm^{-2}.

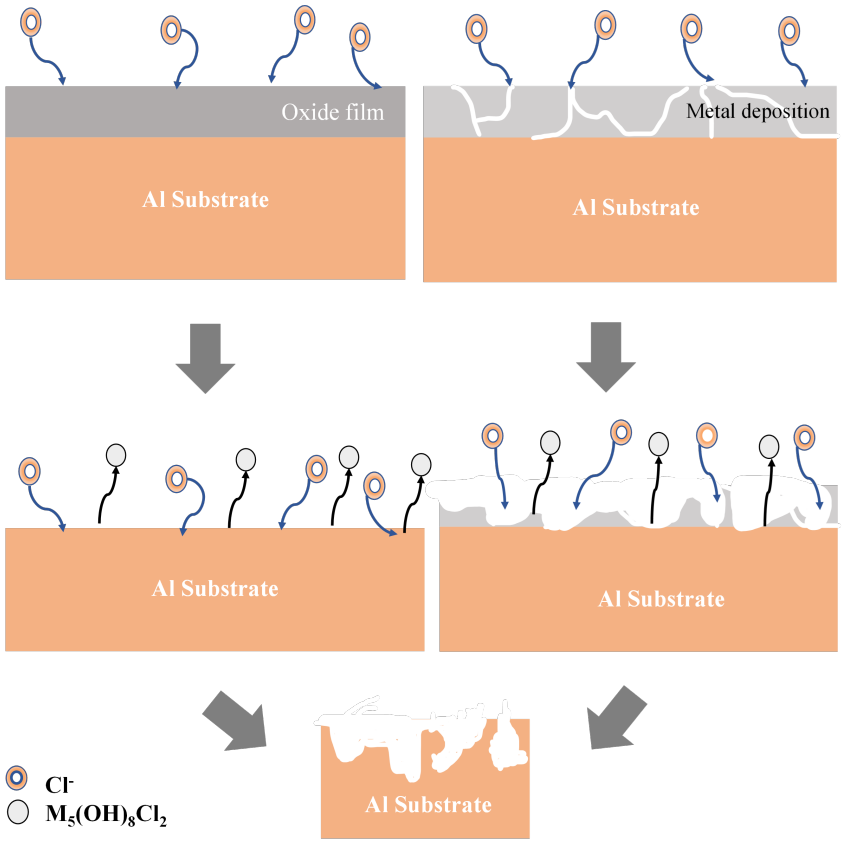


Figure 11. Reaction mechanism of aluminum and coated aluminum in 3.5% sodium chloride.

Another study by Nur'aini et al. reported that Zn can be used as a corrosion inhibitor to improve the electrochemical performance of the anode [43]. The crack formed in the thin layer via electrodeposition onto the Al surface, confirmed by the SEM images above, especially with the EDTA addition variable, also leads the electrolyte to react with the active surface of the anode. Then, the reaction of the anode based on coated aluminum with sodium chloride electrolyte will generate a side product called simonkolleite ($M_5(OH)_8Cl_2 \cdot H_2O$), a white gel with low water solubility. The reaction of the anode in the sodium chloride electrolyte is expressed below:

$$5\,M^{2+} + 8\,OH^- + 2\,Cl^- + H_2O \longrightarrow M_5(OH)_8Cl_2 \cdot H_2O, \quad (1)$$

where M is the metal that reacts with the electrolyte [44].

$$Al + 2\,H_2O \longrightarrow Al_2OH_3 \cdot H_2O + 3\,H^+ + 3\,e^- \quad (2)$$

$$Al_3{}^+ \text{in } Al_2OH_3 \cdot H_2O + Cl^- \longrightarrow Al(OH)_2Cl(\textit{simonkelleite}) \quad (3)$$

Table 4 details the discharge capacities and energies for selected anode samples, highlighting that the aluminum alloy 6061 coated with zinc via EDTA-assisted electrodeposition offers the highest capacity and energy for the Al–air battery. This study indicates that electrodeposition has a significant impact on the anode stability. This is proven with a longer discharge process and more anodic characteristics. Further studies are needed to investigate the possibility of cyclicability, which is the main challenge in battery design employing metal-based materials.

Table 4. Discharge capacity and energy of Al–air battery using 1×1 cm^2 varied anodes.

Anode Sample	Discharge Capacity ($mAh.g^{-1}$)	Discharge Energy ($mWh.g^{-1}$)
Pure Al	0.267	0.11
Zn-pure Al	104.55	60.017
Zn (EDTA)-pure Al	144.501	80.143
AA 6061	94.892	54.466
Zn-AA 6061	247.039	137.109
Zn (EDTA)-AA 6061	414.561	255.077

4. Conclusions

Zinc electrodeposition in both pure aluminum and the aluminum alloy 6061 has been successfully carried out using citrate-based electrolyte solutions, with and without the addition of EDTA. This technique has significantly improved the performance of Al–air batteries by depositing Zn on pure aluminum and the aluminum alloy 6061 with a citrate-based deposition electrolyte solution. Incorporation of EDTA as a chelating agent into the citrate-based deposition electrolyte solution further enhances the performance of the Al–air battery. This improvement is attributed to the facilitated formation of uniform and coherent Zn coatings on the metal surfaces, a benefit not observed in the absence of EDTA.

Specifically, an Al–air battery that comprises an aluminum alloy 6061 anode with Zn electrodeposition, enhanced by the addition of EDTA, paired with a Carbon@MnO_2 cathode and a 3.5% NaCl solution as an electrolyte, has shown exceptional performance. This configuration achieved a specific discharge capacity of 414.561 $mAh.g^{-1}$ and a specific discharge energy of 255.077 $mWh.g^{-1}$, maintaining a stable voltage of 0.55 V for a period of 207 h. This showcases the significant impact of EDTA in promoting electrochemical efficiency and battery longevity.

Author Contributions: Conceptualization, R.B.S. and S.N.; methodology, H.S.; software, S.S.; validation, R.B.S., W.W., and H.S.; formal analysis, S.N.; investigation, S.S.; resources, R.B.S.; data curation, S.N.; writing—original draft preparation, S.N.; writing—review and editing, R.B.S.; visualization, R.B.S.; supervision, H.S.; project administration, W.W.; funding acquisition, R.B.S. All authors have read and agreed to the published version of the manuscript.

Funding: This research received no external funding.

Institutional Review Board Statement: Not applicable.

Informed Consent Statement: Not applicable.

Data Availability Statement: The raw data supporting the conclusions of this article will be made available by the authors on request.

Acknowledgments: The authors would like to express their gratitude to PT. PLN (Persero) and the Sepuluh Nopember Institute of Technology for the completion of this research.

Conflicts of Interest: The authors declare no conflicts of interest.

Abbreviations

The following abbreviations are used in this manuscript:

SEM	Scanning electron microscope
EDX	Energy dispersive X-ray spectroscopy
CV	Cyclic voltammetry
ORR	Oxygen reduction reaction
EDTA	Ethylenediaminetetraacetic acid
PVDF	polyvinylidene fluoride
NMP	N-methyl-2-pyrrolidone
OCP	Open circuit potential

References

1. Mokhtar, M.; Talib, M.Z.M.; Majlan, E.H.; Tasirin, S.M.; Ramli, W.M.F.W.; Daud, W.R.W.; Sahari, J. Recent developments in materials for aluminum–air batteries: A review. *J. Ind. Eng. Chem.* **2015**, *32*, 1–20. [CrossRef]
2. Mohamad, A. Electrochemical properties of aluminum anodes in gel electrolyte-based aluminum-air batteries. *Corros. Sci.* **2008**, *50*, 3475–3479. [CrossRef]
3. Ryu, J.; Park, M.; Cho, J. Advanced technologies for high-energy aluminum–air batteries. *Adv. Mater.* **2019**, *31*, 1804784. [CrossRef] [PubMed]
4. Li, Q.; Bjerrum, N.J. Aluminum as anode for energy storage and conversion: A review. *J. Power Sources* **2002**, *110*, 1–10. [CrossRef]
5. Rahman, A.; Wang, X.; Wen, C. High energy density metal-air batteries: A review. *J. Electrochem. Soc.* **2013**, *160*, A1759–A1771. [CrossRef]
6. Xu, Y.; Zhao, Y.; Ren, J.; Zhang, Y.; Peng, H. An all-solid-state fiber-shaped aluminum–air battery with flexibility, stretchability, and high electrochemical performance. *Angew. Chem.* **2016**, *128*, 8111–8114. [CrossRef]
7. Ma, J.; Li, W.; Wang, G.; Li, Y.; Ren, F.; Xiong, Y. Influences of L-Cysteine/Zinc Oxide Additive on the Electrochemical Behavior of Pure Aluminum in Alkaline Solution. *J. Electrochem. Soc.* **2018**, *165*, A266. [CrossRef]
8. Chen, J.; Xu, W.; Wang, X.; Yang, S.; Xiong, C. Progress and Applications of Seawater-Activated Batteries. *Sustainability* **2023**, *15*, 1635. [CrossRef]
9. Yu, J.; Zhao, C.X.; Liu, J.N.; Li, B.Q.; Tang, C.; Zhang, Q. Seawater-based electrolyte for Zinc–air batteries. *Green Chem. Eng.* **2020**, *1*, 117–123. [CrossRef]
10. Yu, J.; Li, B.Q.; Zhao, C.X.; Zhang, Q. Seawater electrolyte-based metal–air batteries: From strategies to applications. *Energy Environ. Sci.* **2020**, *13*, 3253–3268. [CrossRef]
11. Sun, Z.; Lu, H. Performance of Al-0.5In as Anode for Al–Air Battery in Inhibited Alkaline Solutions. *J. Electrochem. Soc.* **2015**, *162*, A1617. [CrossRef]
12. Lv, C.; Zhang, Y.; Ma, J.; Zhu, Y.; Huang, D.; Li, Y.; Wang, H.; Tang, Y. Regulating Solvation and Interface Chemistry to Inhibit Corrosion of the Aluminum Anode in Aluminum–air Batteries. *J. Mater. Chem. A* **2022**, *10*, 9506–9514. [CrossRef]
13. Tu, J.; Song, W.; Lei, H.; Yu, Z.; Chen, L.; Wang, M.; Jiao, S. Nonaqueous rechargeable aluminum batteries: Progresses, challenges, and perspectives. *Chem. Rev.* **2021**, *121*, 4903–4961. [CrossRef] [PubMed]
14. Lee, W.H.; Choi, S.R.; Kim, J.G. Effect of Agar as Electrolyte Additive on the Aluminum-Air Batteries. *J. Electrochem. Soc.* **2020**, *167*, 110503. [CrossRef]
15. Taeri, O.; Hassanzadeh, A.; Ravari, F. Synergistic Inhibitory Effect of Potassium Sodium Tartrate Tetrahydrate and Sodium Stannate Trihydrate on Self-Corrosion of Aluminum in Alkaline Aluminum-Air Batteries. *Chemelectrochem* **2020**, *7*, 2123–2135. [CrossRef]
16. Cho, Y.J.; Park, I.J.; Lee, H.J.; Kim, J.G. Aluminum anode for aluminum–air battery–Part I: Influence of aluminum purity. *J. Power Sources* **2015**, *277*, 370–378. [CrossRef]
17. Wang, B.; Zhang, L.; Jiang, H.; Li, X.; Mu, X. Atmospheric Corrosion Comparison of Antirust Aluminum Exposed to Industrial and Coastal Atmospheres. *Mater. Corros.* **2018**, *69*, 1516–1525. [CrossRef]
18. Meroueh, L.; Eagar, T.W.; Hart, D.P. Effects of Mg and Si Doping on Hydrogen Generation via Reduction of Aluminum Alloys in Water. *Acs Appl. Energy Mater.* **2020**, *3*, 1860–1868. [CrossRef]
19. Sun, S.; Li, C.L.; Zheng, Q.; Wang, X.M.; Hu, S. The Effect of Environmental Factors on Long-term Atmospheric Corrosion Behavior of Commercially Pure Aluminum AA1035. *Mater. Corros.* **2017**, *68*, 450–457. [CrossRef]
20. Desai, P.S.; Vashi, R.T. Inhibitive Efficiency of Sulphathiazole for Aluminum Corrosion in Trichloroacetic Acid. *Anti-Corros. Methods Mater.* **2011**, *58*, 70–75. [CrossRef]
21. Yu, J.; Hu, Z.; Zexu, D. Electrochemical performance and interface analysis of Al-MgO composite anodes for Al-air batteries. *Journal of The Electrochemical Society* **2020**, *167*, 140514. [CrossRef]
22. Macdonald, D.; Lee, K.; Moccari, A.; Harrington, D. Evaluation of alloy anodes for aluminum-air batteries: Corrosion studies. *Corrosion* **1988**, *44*, 652–657. [CrossRef]
23. Park, I.J.; Choi, S.R.; Kim, J.G. Aluminum anode for aluminum-air battery–Part II: Influence of In addition on the electrochemical characteristics of Al-Zn alloy in alkaline solution. *J. Power Sources* **2017**, *357*, 47–55. [CrossRef]
24. Ma, J.; Wen, J.; Gao, J.; Li, Q. Performance of Al- 1Mg- 1Zn- 0.1 Ga- 0.1 Sn as anode for Al-air battery. *Electrochim. Acta* **2014**, *129*, 69–75. [CrossRef]
25. Wu, Z.; Zhang, H.; Qin, K.; Zou, J.; Qin, K.; Ban, C.; Cui, J.; Nagaumi, H. The role of gallium and indium in improving the electrochemical characteristics of Al–Mg–Sn-based alloy for Al–air battery anodes in 2 M NaCl solution. *J. Mater. Sci.* **2020**, *55*, 11545–11560. [CrossRef]
26. Radošević, J.; Kliškić, M.; Dabić, P.; Stevanović, R.; Despić, A. Processes on aluminium on the negative side of the open-circuit potential. *J. Electroanal. Chem. Interfacial Electrochem.* **1990**, *277*, 105–119. [CrossRef]
27. Deepa, P.; Padmalatha, R. Corrosion behaviour of 6063 aluminium alloy in acidic and in alkaline media. *Arab. J. Chem.* **2017**, *10*, S2234–S2244. [CrossRef]
28. Du, X.; Chen, Y. Corrosion inhibition by a superhydrophobic surface on aluminum that was prepared with a facile electrochemical route. *Mater. Res. Express* **2020**, *7*, 056405.

29. Prakashaiah, B.; Kumara, D.V.; Pandith, A.A.; Shetty, A.N.; Rani, B.A. Corrosion inhibition of 2024-T3 aluminum alloy in 3.5% NaCl by thiosemicarbazone derivatives. *Corros. Sci.* **2018**, *136*, 326–338. [CrossRef]
30. Albasre, N.M.M.; Zakaria, A.; Hussin, M.H. The Study of Electroless Ni-Cu-P Plating on Corrosion Resistance of Aluminium in 3.5% NaCl. *Int. Electroact. Mater.* **2021**, *9*, 12–26.
31. Charitha, B.; Rao, P. Pullulan as a potent green inhibitor for corrosion mitigation of aluminum composite: Electrochemical and surface studies. *Int. J. Biol. Macromol.* **2018**, *112*, 461–472.
32. Mutlu, R.N.; Yazıcı, B. Copper-deposited aluminum anode for aluminum-air battery. *J. Solid State Electrochem.* **2019**, *23*, 529–541. [CrossRef]
33. Zhang, K.; Yan, Z.; Chen, J. Electrodeposition accelerates metal-based batteries. *Joule* **2020**, *4*, 10–11. [CrossRef]
34. Liu, F.; Deng, Y.; Han, X.; Hu, W.; Zhong, C. Electrodeposition of metals and alloys from ionic liquids. *J. Alloy. Compd.* **2016**, *654*, 163–170. [CrossRef]
35. Tang, Y.; Lu, L.; Roesky, H.W.; Wang, L.; Huang, B. The effect of zinc on the aluminum anode of the aluminum–air battery. *J. Power Sources* **2004**, *138*, 313–318. [CrossRef]
36. Zhang, H.; Yuan, J.; Zhu, M. An electrochemical investigation of the EDTA influence on the cobalt-manganese electrodeposition in aqueous chloride electrolytes. *Int. J. Electrochem. Sci.* **2017**, *12*, 8368–8380. [CrossRef]
37. Fashu, S.; Gu, C.D.; Zhang, J.L.; Huang, M.L.; Wang, X.L.; Tu, J.P. Effect of EDTA and NH4Cl additives on electrodeposition of Zn–Ni films from choline chloride-based ionic liquid. *Trans. Nonferrous Met. Soc. China* **2015**, *25*, 2054–2064. [CrossRef]
38. Zhao, Y.; Ren, Y.; Wang, X.; Xiao, P.; Tian, E.; Wang, X.; Li, J. An initial study of EDTA complex based draw solutes in forward osmosis process. *Desalination* **2016**, *378*, 28–36. [CrossRef]
39. Guidelli, R.; Compton, R.G.; Feliu, J.M.; Gileadi, E.; Lipkowski, J.; Schmickler, W.; Trasatti, S. Defining the transfer coefficient in electrochemistry: An assessment (IUPAC Technical Report). *Pure Appl. Chem.* **2014**, *86*, 245–258. [CrossRef]
40. Tian, H.; Li, Z.; Feng, G.; Yang, Z.; Fox, D.; Wang, M.; Zhou, H.; Zhai, L.; Kushima, A.; Du, Y.; et al. Stable, high-performance, dendrite-free, seawater-based aqueous batteries. *Nat. Commun.* **2021**, *12*, 237. [CrossRef]
41. Olabi, A.G.; Sayed, E.T.; Wilberforce, T.; Jamal, A.; Alami, A.H.; Elsaid, K.; Rahman, S.M.A.; Shah, S.K.; Abdelkareem, M.A. Metal-air batteries—A review. *Energies* **2021**, *14*, 7373. [CrossRef]
42. Tsurtsumia, G.; Gogoli, D.; Koiava, N.; Kakhniashvili, I.; Jokhadze, N.; Lezhava, T.; Nioradze, N.; Tatishvili, D. Electrodeposition and characterization of Mn–Cu–Zn alloys for corrosion protection coating electrodeposition and characterization of Mn–Cu–Zn alloys for corrosion PROTECTION coating. *World Multidiscip. Earth Sci. Symp. Ser. Earth Environ. Sci.* **2017**, *95*, 042035.
43. Nur'aini, S.; Susanto, S.; Widiyastuti, W.; Nurtono, T.; Setyawan, H. Unravelling the deposition of Zn and Sn as corrosion inhibitor on aluminum (Al) surface for Al-air battery application with sodium chloride electrolytes. *Mater. Today Proc.* **2024**. [CrossRef]
44. Montiel Guerrero, S.S.; Durmus, Y.E.; Dzieciol, K.; Basak, S.; Tempel, H.; van Waasen, S.; Kungl, H.; Eichel, R.A. Improved Electrochemical Performance of Zinc Anodes by EDTA in Near-Neutral Zinc-Air Batteries. *Batter. Supercaps* **2021**, *4*, 1830–1842. [CrossRef]

Disclaimer/Publisher's Note: The statements, opinions and data contained in all publications are solely those of the individual author(s) and contributor(s) and not of MDPI and/or the editor(s). MDPI and/or the editor(s) disclaim responsibility for any injury to people or property resulting from any ideas, methods, instructions or products referred to in the content.